

Optical properties of Ti, Zr, and Hf from 0.15 to 30 eV

D. W. Lynch and C. G. Olson

Ames Laboratory—USAEC and Department of Physics, Iowa State University, Ames, Iowa 50010

J. H. Weaver

Ames Laboratory—USAEC and Department of Physics, Iowa State University, Ames, Iowa 50010
and Physical Sciences Laboratory,*† University of Wisconsin—Madison, Stoughton, Wisconsin 53589

(Received 28 May 1974)

The absorptivity or reflectivity of polycrystalline samples of Ti, Zr, and Hf was measured from 0.15 to ~30 eV. The data were Kramers-Kronig analyzed to determine the dielectric functions. Between ~0.2 and ~7 eV, each metal showed five structures in the absorptivity and ϵ_2 . These were interpreted as interband transitions within the *d* bands. The ϵ_2 spectra had minima near 7 eV similar to that observed in the bcc transition metals. Additional structures at higher energy could be related to transitions involving highlying bands and the core levels. The electron-energy-loss functions were calculated and discussed in terms of volume and surface plasmons. These metals, like the other transition metals studied, exhibited two volume and two surface plasmons.

INTRODUCTION

The hcp transition metals have received little experimental or theoretical attention in the past years, while the energy bands and Fermi surfaces of many simple and noble metals have been studied extensively. In part, this is because single crystals of purity adequate for Fermi-surface studies are difficult to prepare. For lack of experimental data, theoretical studies have been few and often inconclusive. While one expects the hcp transition metals to be similar to the bcc and fcc transition metals, about which more is known, differences arising primarily from the crystal structure are to be expected. The optical properties, but not the Fermi surfaces, should be qualitatively similar for the different structures.

In the following we report our measurements of the optical properties of Ti, Zr, and Hf in the energy range from 0.15 to ~30 eV. These are compared with our previously reported measurements dealing with the bcc transition metals,^{1,2} and with electron-energy-loss measurements. Structure in ϵ_2 is discussed in terms of existing band calculations.^{3,4}

METHOD

The samples studied were spark cut from ingots which had been prepared by electron-beam melting. They were large and polycrystalline with about 1-mm grains. The Hf sample contained about 1-at.% Zr. The samples were mechanically polished, electropolished (6% perchloric acid in methanol at dry-ice temperature), annealed at ~1150 °C in Ar, and then reelectropolished immediately before being transferred to the sample chambers (time of exposure to air 2–3 min; after 3 min the roughing pumps were started; within 4 min, the vuv chamber pressure was ~5×10⁻³

Torr). At least 50 μm were removed by electropolishing to remove the layer damaged by spark cutting and polishing.^{1,2} Laue x-ray patterns showed sharply defined spots indicating the surface was free of damage.

Data from 0.15 to 4.42 eV were obtained by a calorimetric technique previously described.⁵ The absorptivity *A* was measured at near-normal incidence at 4.2 K with an accuracy of a few percent of the value of *A*. Between 4 and 30 eV, the reflectivity ($R = 1 - A$) was measured using the same samples, but at room temperature. In the region of overlap, the agreement was very good. *R* was measured at 10° angle of incidence with *s*- and *p*-polarized radiation. The high-energy data were taken using the continuum synchrotron radiation from the 240-MeV electron storage ring operated by the Physical Sciences Laboratory of the University of Wisconsin. The apparatus and techniques have been described in detail elsewhere.⁶ The results of the measurements are presented in Figs. 1–6.

Kramers-Kronig (KK) analyses were used to convert the measured spectra to spectra of the complex dielectric function $\tilde{\epsilon} = \epsilon_1 + i\epsilon_2$, from which we calculated the complex refractive index $\tilde{N} = n + ik$, the optical conductivity, the energy-loss functions, and certain sum rules. To perform the KK analyses, it was necessary to introduce high- and low-energy extrapolations. For a free-electron gas, the low-energy absorptivity would be constant and equal to $2/\omega_p\tau$, where ω_p is the plasma frequency and τ is the relaxation time. It was clear from Fig. 1 that interband absorption persisted below 0.2 eV, but the absorption was small and without structure, and Drude-like extrapolations appeared reasonable. The absorptivity at 0.15 eV was set equal to $2/\omega_p\tau$ to determine τ , using the

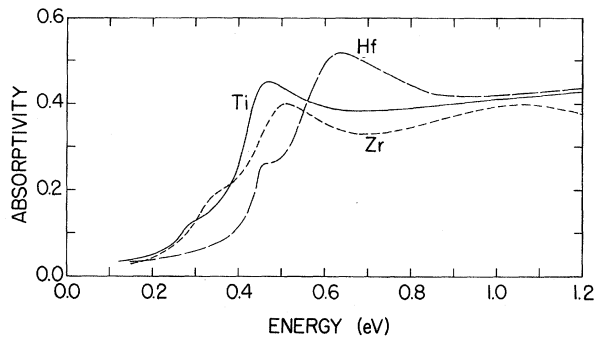


FIG. 1. Absorptivity of Ti, Zr, and Hf at 4.2 K.

free-electron-gas value of ω_p . Then ω_p and τ were used to calculate Drude absorptivities for the extrapolations below 0.15 eV.

The high-energy extrapolations presented more serious problems. For Ti, absorption-coefficient measurements were available⁷ in the 40–310-eV range, and it was possible to calculate R for the extrapolation in that range (assuming $n \approx 1$). For Zr and Hf, such data were not available.

Power-law extrapolations of the form $R(E) = R_0 E^{-\beta}$ are not generally accurate for most materials since transitions from core levels introduce structure in R at high energies. Such extrapolations do, however, give good results if the exponent β can be adjusted to give a known quantity, e.g., ϵ_2 , at one or more selected energies.⁸ This fitting requires independent knowledge of the absolute value of some optical function at one or more energies, either from other measurements or from a theoretical picture that is assumed to apply. There exist so few data on Zr and Hf that such a fitting was not possible.

A requirement of the high-energy extrapolation is that the sum rule on ϵ_2 gives roughly the expected number of core electrons. This sum-rule condition is only approximate since matrix-element effects often make the sum incomplete at the onset

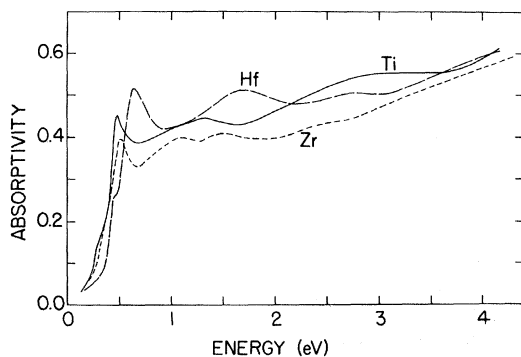


FIG. 2. Absorptivity of Ti, Zr, and Hf at 4.2 K.

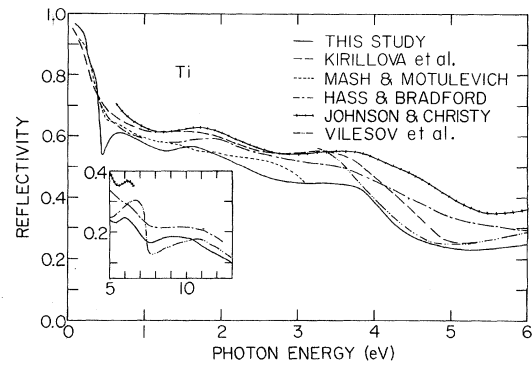


FIG. 3. Reflectivity spectra of Ti obtained in this and other studies. The insert shows the high-energy region.

of transitions from the next deeper core level, but it does place an upper bound on the extrapolated reflectivity.

For the high-energy extrapolations of Zr and Hf, several forms were assumed, and their effect on the dielectric functions in the range of interest was gauged. Attempts were made to account for the presence of core transitions related to the 4s levels of Zr,⁹ and the 5s and 5p levels of Hf.⁹ At higher energies, our ultimate extrapolation had a power-law form with the choice of β determined by the sum-rule condition and experience with other bcc metals.^{1,2} For Zr, absorption due to the 3d, 4s, 4p, and 4d electrons would be (approximately) exhausted by 200 eV,⁹ and the sum rule would give 22 electrons per atom ($\bar{\nu}$). A β of 3.5 above 60 eV gave 21 $\bar{\nu}$ at 200 eV for Zr. For Hf, 14 additional 4f electrons would raise N_{eff} to 36 near 250 eV.⁹ A β of 3 above 40 eV gave 35 $\bar{\nu}$. The effect of different β 's was that for Hf, for example, $\beta=3.5$ gave only 21 $\bar{\nu}$ while a by-eye extrapolation with roughly $\beta=4.4$ caused ϵ_2 to be negative between ~ 50 and 300 eV. While different β 's produced

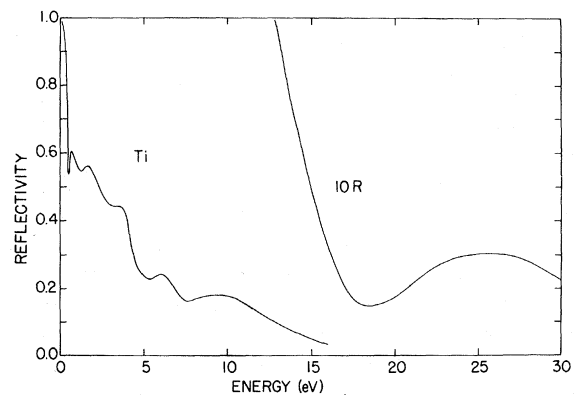


FIG. 4. Reflectivity of Ti. The high-energy region has been expanded for clarity.

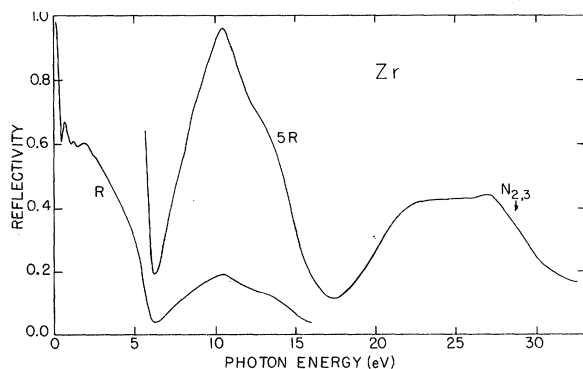


FIG. 5. Reflectivity of Zr. The high-energy region has been expanded for clarity. Core levels have been placed according to their atomic energies (Ref. 9).

large changes at high energy, their effects in the region of interest were smaller: The difference in ϵ_2 between $\beta=3.0$ and 3.5 for Hf was 1.8% (1 eV), 3.5% (5 eV), 2.5% (10 eV), -1% (20 eV with ϵ_2 for $\beta=3.5$ being greater), and 2.1% (25 eV). Finally, for Ti the experimental results⁷ between 70 and 300 eV could be approximated by $\beta=3.7$ ($3p$ levels lie near 45 eV). To account for the added absorption in Zr and Hf, β must be decreased, and our choices were reasonable.

The problem of oxide formation on crystalline samples prepared in air and transferred to a sample chamber is one which particularly plagues *in situ* studies. In the infrared, the oxides tend to be transparent and have negligible effects. In the visible, the effects of a transparent oxide become greater (because of the values of n and k of the metal), and in the ultraviolet, where the oxide is absorbing, qualitative as well as quantitative effects can occur. In general, the effect of a thin, transparent oxide layer is to reduce the reflectivity.¹⁰

In this study we have made no effort to correct for an oxide layer since the oxide could not be assumed to be transparent. A correction for an absorbing oxide would be reliable only if its thickness, uniformity, and nature were known. Since several oxides exist for these metals and since the oxidation rates vary for different crystal faces, such corrections would have little meaning. Finally, the optical properties of the transition-metal oxides are not generally known at high energy.

Ti is the most reactive of our samples and numerous runs were made with this sample (always freshly electropolished). All spectra were qualitatively similar to the curve shown in Fig. 3, but for some the magnitudes of R were lower. The effect of electropolishing was to increase R and sharpen structure as the surface quality improved. A point was reached, however, beyond which fur-

ther electropolishing did not change R , and the magnitudes were then reproducible from one run to the next to within 5% of the magnitude of R . Since we were unable to study the sample surface quality *in situ*, a more quantitative estimate of the effect of the surface contamination of our Ti in the vuv is not possible. Since Zr and Hf oxidize much more slowly, the effects of oxides for those metals were probably small.

This study represents the first examination of Ti and Zr over a wide energy range. To our knowledge, Hf has not been studied before by optical techniques. Since the samples were not oriented single crystals, the calculated dielectric functions must represent an average dielectric function and any anisotropy of the dielectric tensor must be determined at a later time.

DISCUSSION

We first compare our data with those in the literature. Kirillova and co-workers¹¹⁻¹³ measured the optical constants of polycrystalline samples of Ti that had been mechanically polished in acid. They used an ellipsometric method and covered the 0.06-5-eV range at room temperature. The reflectivity spectrum calculated from their values of n and k is shown in Fig. 3. The prominent minimum we find in R at 0.465 eV is absent, although their data show a slope change there. The weaker minimum at 1.3 eV is also absent. More recently, Mash and Motulevich¹⁴ made ellipsometric measurements ($\sim 0.1-3$ eV at 300 K) on electropolished samples similar to ours. They showed that below 3 eV the effect of oxidation was to change n and k by only 2-5% after 3 days.

Hass and Bradford¹⁵ measured the reflectivity of evaporated films of Ti ($\sim 10^{-6}$ Torr) between ~ 0.1 and ~ 12.5 eV. They reported a few ellipsometric measurements in the visible, and described a study of the effects of a buildup of an oxide layer during exposure to air. Their results indicated

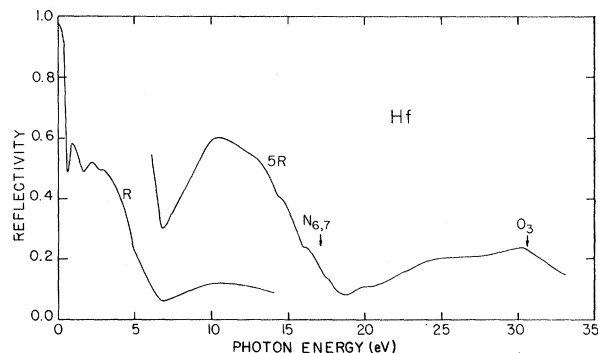


FIG. 6. Reflectivity of Hf. The high-energy region has been expanded for clarity. Core levels have been placed according to their atomic energies (Ref. 9).

TABLE I. Energy positions of structure in the reflectivities of Ti, Zr, and Hf. Additional features in Zr and Hf can be related to core structure (see Table II and text). All energies are in eV.

	Ti	Zr	Hf
Shoulder in $1-R$	0.3	0.34	0.45
Minimum	0.465	0.51	0.615
Maximum	0.67	0.68	0.92
		1.10	
Minimum	1.27	1.26	1.7
Maximum	1.6	1.5	2.2
		1.9	
Minimum	2.9	2.4	2.75
Maximum	3.8	2.65	2.95
Minimum	5.3	3.4	5.0
Maximum	6.0		
Minimum ^a	7.7	6.24	6.85
Maximum	9.3	10.5	10.5
Minimum	18.5	17.4	18.8

^aMarks the onset of high-energy absorption.

that a 17-Å film of TiO₂ formed within ~2 hours (room temperature) after the film deposition was completed. The oxide continued to grow and reached ~35 Å after 60 days. Since our crystals were exposed to air much less than 2 hours, we can assume that we have considerably less than 17 Å of oxide cover, particularly since crystals tend to oxidize more slowly than films. The reflectivity spectrum of Hass and Bradford is shown in Fig. 3.

Johnson and Christy¹⁰ measured the transmission and reflection of evaporated Ti films in the 0.6–

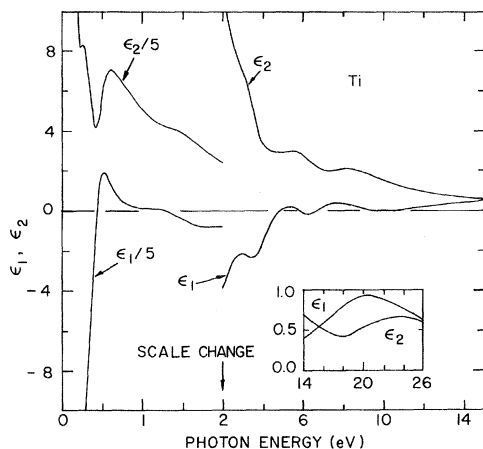


FIG. 7. Real and imaginary parts of the dielectric function of Ti. The energy scale is linear but it changed at 2 eV.

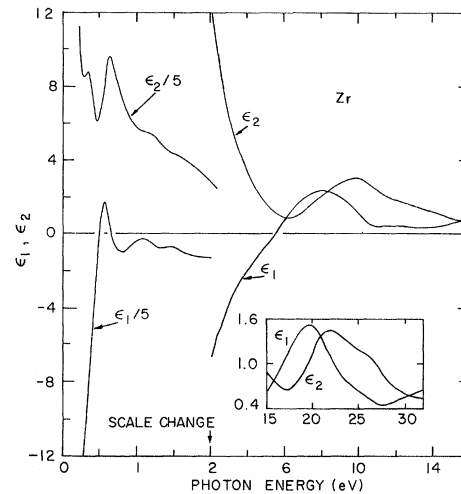


FIG. 8. Real and imaginary parts of the dielectric function of Zr. The energy scale in linear but it changed at 2 eV.

6.6-eV range at room temperature. The films were evaporated in a vacuum of about 10^{-7} Torr and kept in a nitrogen atmosphere during the measurements. The reflectivities calculated from their values of n and k are consistently higher than ours, but the qualitative agreement is good.

Several groups¹⁶⁻¹⁸ have studied Ti at one or two wavelengths in the visible. Menard¹⁶ used a mechanically polished sample while Smith¹⁷ used a sample annealed *in situ*. Carroll and Malmed¹⁸ compared a chemically polished sample to an ultra-high-vacuum film. The results of these studies lie within the spread of Fig. 3. Finally, Vilesov *et al.*¹⁹ measured the reflectivity of mechanically and chemically polished samples of Ti by a novel photoemission method, covering the range from about 3 to 15 eV. Their data, also presented by Kirillova *et al.*,²⁰ have roughly the same shape as ours, but their peak near 6 eV is more pronounced and appears at higher energy.

Zr has been studied less frequently than Ti. Kirillova *et al.*^{12,20} reported ellipsometric measurements between 0.06 and 5 eV, but the agreement with our results is only fair. They showed broad minima in R near 1 and 2.5 eV. Vilesov *et al.*¹⁹ also measured the reflectivity of Zr, but the structures in their spectra are very different from ours. No optical data on Hf were found. Table I gives a summary of our reflectivity spectra.

Figures 7-9 show the real and imaginary parts of the dielectric function for Ti, Zr, and Hf determined from our KK analyses. The low-energy interband absorption in these metals lies from a few tenths of an eV to about 7 eV, the lower region being superimposed on a free-electron background.

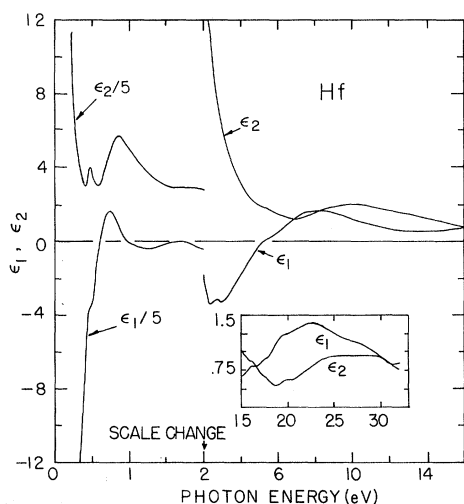


FIG. 9. Real and imaginary parts of the dielectric function of Hf. The energy scale in linear but it changed at 2 eV.

The results are summarized in Table II. Ti and Hf show five features below about 7 eV with Zr having a sixth. These are shown somewhat more clearly in the optical conductivity, $\sigma = \epsilon_2 \omega / 4\pi$ (Fig. 10).

The over-all strong interband absorption is similar to that in the bcc transition metals,^{1,2} absorption arising from transitions from filled parts of the *d* bands to empty parts of the *d* bands. (The bands are certainly hybridized with *s* and *p* character, but the position in energy of the strong ab-

TABLE II. Position of maxima in ϵ_2 for Ti, Zr, and Hf. All energies are in eV.

Ti	Zr	Hf
0.28	0.35	0.47
0.62	0.64	0.85
1.45	1.20	1.8
	1.58	
3.2 ^a	2.6 ^a	2.7 ^a
5.6	4.0 ^b	5.2
8.2	9.9	10.0
	13.0	
23.8	21.9	22.5
		14.5 ^d
	26.4 ^c	16.1
		17.5
		19.3
		28.5 ^e

^aBetter seen in the conductivity (Fig. 10).

^bSubtle feature in conductivity corresponding to broad, weak absorption as seen in *R* (Fig. 5).

^c*N*_{2,3} core structure (see text).

^d*N*_{6,7} core structure (tentative identification—see text).

^e*O*_{2,3} core structure (see text).

sorption requires it to arise from filled and empty states, all in the “*d*-band region” of the density of states.) The very sharp structure in Fig. 10 is not shared with the bcc metals with the exception perhaps of W. However, there should be a characteristic difference in the band structures for the two lattices, with perhaps more prominent parallel bands cutting the Fermi level in the hcp structure. It should be borne in mind that our spectra are for polycrystalline samples; the spectra of the individual components of the conductivity tensor may be even sharper.

Energy bands have been calculated for Ti,⁴ but these have not been fit to experimental data, and any assignments would be rather tenuous. In the absence of extensive energy-band calculations for Hf, the assignment of the structure in ϵ_2 to regions of *k* space is not possible. While detailed calculations of the band of hcp Re are available,²¹ the application of these via a rigid-band model to Ti, Zr, and Hf does not appear warranted. Small shifts in the bands near the Fermi level could dramatically change the predicted optical structure. Further, the sharp structure we have observed at low energy might be due to small regions of *k* space removed from the symmetry lines usually for reporting band structures. It is hoped that this optical study and other Fermi-surface studies²²⁻²⁴ will stimulate interest in the electronic properties of these metals.

Recently, the energy bands and the joint density of states of Zr were calculated by Myron.²⁵ There is considerable agreement between the structures in the conductivity, calculated with the constant-matrix-element approximation, and the structures in Fig. 10. A small calculated peak at 0.35 eV corresponds to our peak at 0.37 eV. It arises from transitions between nearly parallel bands around Γ (along *T* and Σ) through which the Fermi level passes. Subsequent calculated conductivity peaks appear at 0.9, 1.5, 1.8, and 2.3 eV. The

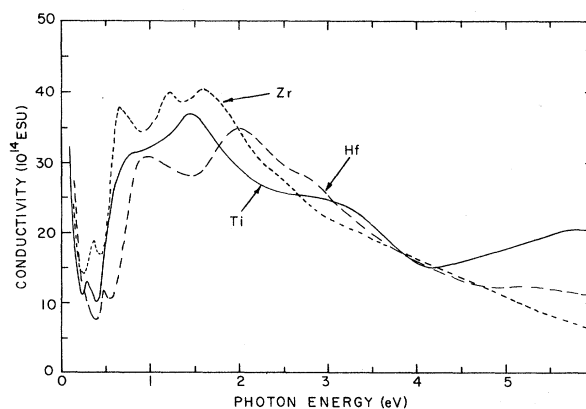


FIG. 10. Conductivity of Ti, Zr, and Hf.

first is surely our peak at 0.66 eV, and it arises from transitions between nearly parallel bands along *S*. The correlation of the calculated structures at 1.5, 1.8, and 2.3 eV with the experimental features at 1.22 and 1.6 eV is less certain. The calculated peak at 1.5 eV arises from parallel-band transitions along *P*, that at 1.8 eV from parallel bands along *U*, and that at 3.4 eV from parallel bands along *S*. This will be discussed in more detail when the calculations are reported.²⁵

The hcp metals, like the bcc and fcc²⁶ transition metals, possess the characteristic minimum in ϵ_2 above the first absorption band. In the bcc metals, this minimum appears at about 10 eV. Above the minimum, a second wide, structured absorption band appears which has been attributed to transitions from occupied states to final states ≈ 10 eV above E_F . These final states correspond to the 7th and higher-lying bands which have largely *s*, *p* and *f* character and a high density of states. While no calculations of the joint density of states or ϵ_2 have extended to these high photon energies, it appears reasonable to attribute this high-energy structure to such transitions. This assignment is supported by recent high-energy thermoreflectance studies of Au.²⁷ From our optical measurements of the hcp metals, the high-lying, flat bands should be placed closer to E_F than for the bcc or fcc metals, but more detailed assignments must await further theoretical efforts.

Structure has been observed in the reflectivity and dielectric-function spectra which can be related to transitions involving core states. The 4*p* levels of Zr have been placed near 28.7 eV,⁹ and observed structure in ϵ_2 near 26.4 eV can be related to those $N_{2,3}$ levels. Similarly, for Hf the 4*f* states which lie about 17.1 eV⁹ below E_F might be responsible for the four structures observed in ϵ_2 at 14.5, 16.1, 17.5, and 19.3 eV, though the structures are surprisingly strong for *f*-*d* tran-

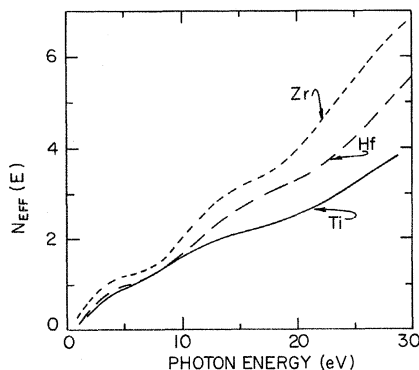


FIG. 11. N_{eff} calculated from the oscillator-strength sum rule. See text for discussion of the low-energy region.

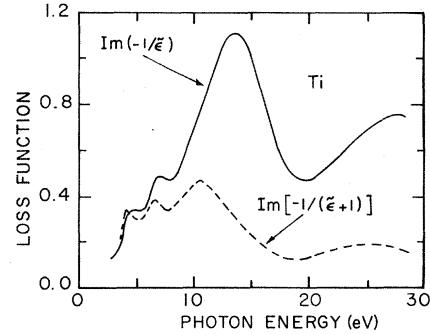


FIG. 12. Volume $\{\text{Im}[-1/\bar{\epsilon}]\}$ and surface $\{\text{Im}[-1/(\bar{\epsilon}+1)]\}$ loss functions of Ti.

sitions. The $O_{2,3}$ levels are probably responsible for the structure observed at 28.5 eV in Hf. For Ti, the core levels lie outside the range of our measurements.

Figure 11 shows the result of the partial sum rule

$$N_{\text{eff}}(E) = \frac{2}{\pi} \frac{1}{(\hbar\omega_p)^2} \int_{0.1 \text{ eV}}^E \epsilon_2(E') E' dE',$$

where $\hbar\omega_p$ is the free-electron-plasma energy. $N_{\text{eff}}(E)$ is the number of electrons per atom contributing to absorption between 0.1 eV and E . There is considerable oscillator strength from the valence electrons over the entire range from 0.1 to 30 eV with additional strength coming from core levels as identified above. Note that the contribution to the integral below 0.1 eV has not been included in Fig. 11. (It is very sensitive to the free-electron-gas parameters used to describe the region below 0.1 eV, being $(8/\pi)(m_0/m^*) \tan^{-1} [(0.1 \text{ eV})\tau/\hbar]$ for these metals, where m^* is a conductivity effective mass and τ an electron relaxation time.)

Figures 12–14 show the loss functions for volume and surface plasmons, $\text{Im}(-1/\bar{\epsilon})$ and $\text{Im}[-1/(\bar{\epsilon}+1)]$, respectively. Peaks in these occur at energies corresponding to the energies a fast electron would lose in exciting a volume and surface plasmon, respectively. There can also be peaks due to interband and core transitions, but these can usually be identified by comparison with structure in ϵ_2 . The plasmon peaks will occur where ϵ_2 is small and structureless. Ti, Zr, and Hf, like the bcc^{1,2} and fcc²⁶ metals, exhibit two volume plasmons and two surface plasmons. The results are summarized in Table III. The higher-energy volume plasmon occurs at an energy close to the free-electron value, determined by using the number of *s*, *p*, and *d* electrons and the free-electron mass. Exact agreement is not expected because of the occurrence of nearby interband and core transitions. The lower-energy volume plasmons seem

less damped than their counterparts in the bcc metals.^{1,2} None of these bear a $\sqrt{2}$ relationship to the volume-plasmon energies, as expected for a free-electron gas, but these are much more complicated systems.

There is some previous work on electron-energy-loss measurements in Hf. Lynch and Swan²⁸ found loss peaks at 7.7, 15.9, and 33.4 eV in Hf, the 15.9-eV peak corresponding to our bulk-plasmon peak at 15.8 eV combined with the nearby core features (see Fig. 14). The 33.4-eV peak is probably a composite of the O_2 and O_3 core-level excitations. Their low-energy structure probably corresponds to our structure near 6 eV. This latter structure is seen to be a combination of the interband feature at ~ 5.2 eV and the low-energy plasmon.

Lynch and Swan also measured energy-loss spectra in Zr, finding peaks at 8.0, 14.6, and 28.7 eV. Our volume-loss function also shows a strong peak at 28.8 eV which is probably due to the excitation of the $N_{2,3}$ core levels. The 15.6-eV peak corresponds to our volume plasmon at 14.6 eV. Rudisil *et al.*²⁹ reported measuring the plasma frequency in Zr by looking for a plasma edge in the transmission of thin films. The edge observed gives a plasmon energy of 15.7 eV.

The situation in Ti is more complicated. The measurements of Robins and Swan³⁰ gave electron-energy-loss peaks at 5.5 and 17.6 eV. Later Best³¹ measured Ti that had been exposed to a low pressure of oxygen, getting electron-energy-loss peaks at 6.3, 11.4, 19.5, and 25 eV. More recently, Simmons and Scheibner³² measured electron-energy-loss peaks at 5.0, 11.5, 17.0, and 24.6 eV on clean Ti surfaces. Subsequent exposure to oxygen removed the 5.0- and 17.0-eV

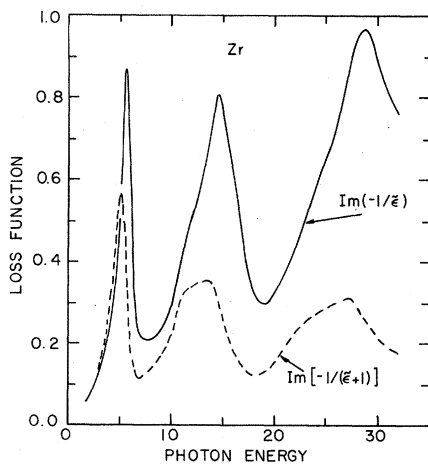


FIG. 13. Volume $\{\text{Im}(-1/\bar{\epsilon})\}$ and surface $\{\text{Im}[-1/(\bar{\epsilon}+1)]\}$ loss functions of Zr.

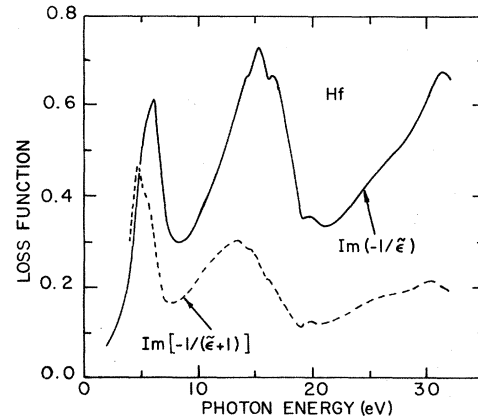


FIG. 14. Volume $\{\text{Im}(-1/\bar{\epsilon})\}$ and surface $\{\text{Im}[-1/(\bar{\epsilon}+1)]\}$ loss functions of Hf.

peaks from the spectra, and left the other two at the same positions. The peaks that were removed were attributed to surface plasmons and those that remained to volume plasmons, although the 17.0- and 24.6-eV peaks were attributed to double excitations. The alternation of surface and volume plasmons with increasing energy, shown in Fig. 12, makes Ti similar to Zr and Hf, but there is considerable disagreement in the values of the energies of the plasmons between Simmons and Scheibner, our data, and the earlier energy-loss data.

CONCLUSION

The optical properties of Ti, Zr, and Hf have been reported over a wide energy range, and discussed in terms of interband transitions at low energy, transitions to high-lying states above 7 eV, core-level excitations, and plasmon effects. The discussion has had to be rather qualitative in the absence of extensive band calculations, but it is hoped that these measurements will generate additional theoretical interest. Finally, it has been shown that these hcp transition metals have considerable similarities with their bcc and fcc neighbors, notably the double plasmons and high-lying interband absorption.

TABLE III. Position of maxima in volume and surface loss functions of Ti, Zr, and Hf. $\hbar\omega_p$ is the free-electron-plasma energy (see text). All energies are in eV.

	Ti	Zr	Hf
$\hbar\omega_p$	17.6	15.4	15.8
Volume	13.7	14.6	15.3
Surface	10.7	13.4	13.4
Volume	4.7	5.7	6.1
Surface	4.2	5.2	4.7

Larger figures or tables can be obtained from the authors.

ACKNOWLEDGMENTS

The authors wish to acknowledge F. A. Schmidt for providing the starting ingots and annealing the

samples, and H. H. Baker for assistance in the electropolishing processes. H. W. Myron generously provided the results of his band calculations of Zr prior to their publication. The cooperation of the storage-ring staff, especially E. M. Rowe, C. H. Pruett, and R. A. Otte is appreciated.

*Permanent address.

[†]Storage ring was supported by U. S. Air Force Office of Scientific Research under Contract No. F44620-70-0029.

¹J. H. Weaver, D. W. Lynch, and C. G. Olson, *Phys. Rev. B* **7**, 4311 (1973).

²J. H. Weaver, D. W. Lynch, and C. G. Olson, *Phys. Rev. B* **10**, 501 (1974).

³S. L. Altmann and C. J. Bradley, in *Soft X-Ray Band Spectra*, edited by D. J. Fabian (Academic P., New York, 1968).

⁴R. M. Welch and E. H. Hygh, *Phys. Rev. B* **1**, 2424 (1970); 4261 (1971); 1993 (1974).

⁵L. W. Bos and D. W. Lynch, *Phys. Rev. B* **2**, 4784 (1970).

⁶C. G. Olson and D. W. Lynch, *Phys. Rev. B* **9**, 3159 (1974).

⁷B. Sonntag, R. Haensel, and C. Kunz, *Solid State Commun.* **7**, 597 (1969); B. Sonntag (unpublished).

⁸P. O. Nilsson and L. Munkby, *Phys. Kondens. Mater.* **10**, 290 (1969).

⁹J. A. Bearden and A. F. Burr, *Rev. Mod. Phys.* **39**, 125 (1967).

¹⁰P. B. Johnson and R. W. Christy, *Phys. Rev. B* **9**, 5056 (1974).

¹¹G. A. Bolotin, A. N. Voloshinskii, M. M. Kirillova, M. M. Noskov, A. V. Sokolov, and B. A. Charikov, *Fiz. Metal. Metalloved.* **13**, 823 (1962) [*Phys. Met. Metallogr.* **13**, No. 6, 24 (1962)].

¹²M. M. Kirillova and B. A. Charikov, *Fiz. Metal. Metalloved.* **15**, 315 (1963) [*Phys. Met. Metallogr.* **15**, No. 2, 138 (1963)].

¹³M. M. Kirillova and B. A. Charikov, *Fiz. Metal. Metalloved.* **19**, 495 (1965) [*Phys. Met. Metallogr.* **19**, No. 4, 13 (1965)].

¹⁴I. D. Mash and G. P. Motulevich, *Zh. Eksp. Teor. Fiz.* **63**, 985 (1972) [*Sov. Phys.-JETP* **36**, 516 (1973)].

¹⁵G. Hass and A. P. Bradford, *J. Opt. Soc. Am.* **47**, 125 (1957).

¹⁶R. C. Menard, *J. Opt. Soc. Am.* **52**, 427 (1962).

¹⁷T. Smith, *J. Opt. Soc. Am.* **62**, 774 (1972).

¹⁸J. J. Carroll and A. J. Melmed, *J. Opt. Soc. Am.* **64**, 514 (1974).

¹⁹F. I. Vilesov, A. A. Azgrubskii, and M. M. Kirillova, *Opt. Spektrosk.* **153** (1967) [*Opt. Spectrosc.* **23**, 79 (1967)].

²⁰M. M. Kirillova, L. V. Nomerovannaya, G. A. Bolotin, V. M. Mayevskiy, M. M. Noskov, and M. S. Bolotina, *Fiz. Metal. Metalloved.* **25**, 459 (1968) [*Phys. Met. Metallogr.* **25**, No. 3, 81 (1968)].

²¹L. F. Mattheiss, *Phys. Rev.* **15**, 459 (1966).

²²J. E. Schirber, *Phys. Lett. A* **33**, 172 (1970).

²³A. C. Thorson and A. S. Joseph, *Phys. Rev.* **131**, 2078 (1963).

²⁴P. M. Everett, *Phys. Rev. B* **6**, 3553 (1972); **6**, 3559 (1972).

²⁵H. W. Myron (private communication).

²⁶See J. H. Weaver (unpublished).

²⁷C. G. Olson, M. Piacentini, and D. W. Lynch, *Phys. Rev. Lett.* **33**, 644 (1974).

²⁸M. J. Lynch and J. B. Swan, *Aust. J. Phys.* **21**, 811 (1968).

²⁹J. E. Rudisil, A. Matsui, and G. Weissler, *Opt. Commun.* **2**, 39 (1970).

³⁰J. L. Robins and J. B. Swan, *Proc. Phys. Soc. Lond.* **76**, 857 (1960).

³¹P. E. Best, *Proc. Phys. Soc. Lond.* **80**, 1308 (1962).

³²G. W. Simmons and E. J. Scheibner, *J. Appl. Phys.* **43**, 693 (1972).